Journal of the European Ceramic Society **12** (1993) 185–195

Al_2O_3/Al Composites Formed by the Directed Oxidation of an Al–Mg–Zn Alloy

Ping Xiao & Brian Derby

Department of Materials, University of Oxford, Parks Road, Oxford OX1 3PH, UK

(Received 21 December 1992; accepted 19 March 1993)

Abstract

Al_2O_3/Al composites have been produced by the directed oxidation of an Al-2·2 at% Mg-2·2 at% Zn alloy. Thermal gravimetric analysis was used to characterise the reaction kinetics. The resulting microstructure was characterised using optical microscopy and scanning electron microscopy coupled with EDX and WDX microanalysis. Rapid oxide growth occurs in the temperature interval 1100°C < T < 1400°C with the upper temperature controlled by the rate of Mg loss from the system. The reaction is controlled by the presence of a Mg concentration at the composite/air interface. The Mg content in a network of molten Al feeder channels is maintained at 0·2 at% Mg with a thick spinel layer at the alloy/Al_2O_3 interface. These are shown to be consistent with theoretical calculations of phase equilibria in the Al–Mg–O system. The spinel acts as a buffer controlling the Mg level in the channels. Also from the equilibria at 1200°C it is likely that the Mg at composite/air interface exists in the form of $MgAl_2O_4$.

Al_2O_3/Al-Verbundwerkstoffe wurden durch die direkte Oxidation einer Al-2·2 At.% Mg-2·2 At% Zn-Legierung hergestellt. Die Reaktionskinetik wurde gravitometrisch charakterisiert und das resultierende Mikrogefüge mit Hilfe der Licht- und Rasterelektronenmikroskopie (verbunden mit EDX und WDX) untersucht. Ein schnelles Oxidwachstum erfolgt im Temperaturbereich 1000°C < T < 1400°C, wobei die untere Grenztemperatur durch das Ausmaß des Mg-Verlustes des Systems bestimmt wird. Die Reaktion wird durch die Mg-Konzentration an der Verbund/Luft-Grenzfläche bestimmt. Ein Mg-Gehalt von 0·2 At.% in dem Netzwerk geschmolzener Al-Zuführungskanäle wird durch eine dicke Spinellschicht an der Legierung/Al_2O_3-Grenzfläche aufrechterhalten. Es wird gezeigt, daß dies mit theoretischen Berechnungen der Phasengleichgewichte des Al–Mg–O-Systems in Übereinstimmung ist. Der Spinell wirkt dabei wie ein Puffer, der die Mg-Konzentration in den Kanälen regelt. Aus den Gleichgewichten bei 1200°C läßt sich schließen, daß das Mg an der Verbund/Luft-Grenzfläche wahrscheinlich in der Form $MgAl_2O_4$ vorliegt.

Des composites Al_2O_3/Al ont été produits par oxydation directe d'un alliage ternaire d'Al–Mg (2·2% at)–Zn (2·2% at). L'analyse thermique gravimétrique a été utilisée pour caractériser les vitesses de réaction. La microstructure a été caracterisée au moyen de la microscopie optique et de la microscopie à balayage électronique couplée avec des microanalyses EDX et NDS. Une croissance rapide d'oxyde apparaît dans l'intervalle de température de 1100°C à 1400°C, où la température supérieure est contrôlée par le taux de Mg perdu par le système. La réaction est contrôlée via la présence d'une concentration en Mg à l'interface composite-air. La teneur en Mg dans un réseau de canaux d'alimentation d'Al en fusion est maintenue à 0·2% atomique avec une épaisse couche de spinelle à l'interface alliage/Al_2O_3. Ceux-ci paraissent compatibles avec les calculs théoriques d'équilibre de phase dans le système ternaire Al–Mg–O. Le spinelle agit comme tampon en contrôlant le niveau de Mg dans les canaux. Egalement à partir du diagramme de phase à 1200°C, il est vraisemblable que le Mg à l'interface composite/air existe sous la forme de $MgAl_2O_4$.

1 Introduction

Certain molten aluminium alloys can be rapidly oxidised by vapour phase oxidants to produce oxide/metal composites in a limited temperature range. This is known as directed metal oxidation. Initial studies considered the formation of Al_2O_3 composites by the oxidation of a molten Al–Mg–Si alloy.[1] Mg and Si concentrations ranged from 1 to

Journal of the European Ceramic Society 0955-2219/93/$6.00

10 wt% and the growth was largely confined to temperatures in the range 1100°C–1400°C. The presence of both Mg and Si in the alloy was considered necessary for the reaction. Mg was believed to act as an initiator of the reaction and Si as a stabilising agent to ensure the continuation of oxidation.[1,2] It was reported that the action of Si could be duplicated by all the group IV elements (Si, Ge, Sn, Pb) and that the presence of one of these elements in addition to Mg was necessary to promote directed oxidation. Since then simple Al–Mg alloys have been used for the directed oxidation experiments but in this case the reaction was initiated by scratching the surface of the alloy exposed to air prior to heating.[3] Mg-free Al alloys containing Si and Zn can also be used to initiate the directed oxide growth so long as the molten alloy is in contact with bulk $MgAl_2O_4$.[4]

The microstructure and microstructural development of Al_2O_3/metal composites formed by the directed oxidation of a molten metal have been reported in the past.[1,2,5–7] The composite, in the absence of a filler, was characterised by:

(i) A preferred orientation of the interconnected Al_2O_3 perpendicular to the plane of the original alloy surface and a growth direction [0001].
(ii) Columnar regions in which low-angle Al_2O_3/Al_2O_3 grain boundaries predominate.
(iii) A band of $MgAl_2O_4$ at the interface between the composite and the original alloy surface.
(iv) Partially interconnected microscopic metal channels about 3–5 μm in diameter running through the length of the material.

Antolin & Nagelberg[5] and Salas *et al.*[8] investigated the growth of Al_2O_3/metal composites by the directed oxidation of molten Al–Mg–Si alloys. During the early stages of oxidation a MgO-covered $MgAl_2O_4$ layer is formed and thickens. The growth initiation is marked by the spread of a metal-rich zone over the duplex oxide layer. During the growth process, a layered structure was proposed at the upper extremity of the composite, consisting of MgO at the top surface, $MgAl_2O_4$, Al alloy, and finally the bulk Al_2O_3 composite containing microchannels of the alloy. Salas *et al.*[8] reported that the typical oxidation sequence consists of an initial event of rapid but brief oxidation, followed by an incubation period of limited oxide growth after which the bulk Al_2O_3/Al composite forms. Nagelberg[9,10] reported a study of the kinetics of oxidation of an Al–Mg–Si alloy and a more complex Al–Si–Zn–Cu–Fe–Mg alloy which produced conflicting results. Using a combination of DTA and TGA techniques the activation energy of oxidation of the Al–Mg–Si alloy was measured as 400 kJ mol^{-1} with a dependence of the reaction rate on oxygen partial pressure of $P(O_2)^{-1/4}$, and an activation energy of 89 kJ mol^{-1} with no effect of oxygen partial pressure for the Al–Si–Zn–Cu–Fe–Mg alloy. These contradictory results occur despite both alloys giving essentially identical microstructures after oxidation. Vlach *et al.*[11] also reported a thermogravimetric study of the oxidation of an Al–Mg–Si alloy. After the incubation period, the composite growth typically involves two sequential regimes: an initial period of accelerating growth, and subsequent deceleration showing approximately parabolic dependence on time. The growth rate increased with temperature to a maximum at ~1300°C, with a nominal activation energy of 270 kJ/mol for an Al-2·85 wt% Mg-5·4 wt% Si alloy in O_2 at furnace temperatures of 1000–1300°C. An oscillatory rate regime observed at 1000–1075°C resulted in a banded structure of varying Al_2O_3-to-metal volume fraction.

The majority of these previous studies focused on the study of the directed oxidation of Al–Mg–Si. There have been a few investigations of other reaction systems but there has been little detailed research on them. The exact function of the dopants is unclear. Early work considered the addition of Si as necessary,[1] but since then this has been shown to be false.[3] In this paper an Al-2·2 at% Mg-2·2 at% Zn alloy was used in directed oxidation experiments. Thermogravimetric analysis was used to measure weight gain and reaction rate. Optical microscopy and scanning electron microscopy (SEM) coupled with microanalysis using energy and wavelength dispersive spectroscopy (EDS and WDS) have been used to characterise the resulting microstructures.

2 Experimental work

Oxidation experiments were carried out in air. Short cylindrical specimens of Al-2·2 at% Mg-2·2 at% Zn alloy were machined and inserted into slightly larger crucibles of 99·9 wt% purity Al_2O_3. The crucible was inserted into a vertical tube furnace. A laboratory microbalance with 0·1 mg accuracy was used to monitor the specimen's weight continuously. The specimens were hung from a nichrome or Pt wire in the centre of the tube furnace at temperatures up to 1400°C. Measurement started immediately after the specimen was inserted into the preheated vertical tube furnace. A continuous record of weight gain was made during the process.

After removal from the furnace, partially or completely oxidised specimens were sectioned for optical, SEM, TEM and electron probe microanalysis. Microanalysis of polished sections was carried out on a Cameca Camebax electron microprobe using wavelength dispersive spectroscopy. All optical and SEM micrographs were taken on a plane parallel to the growth direction. The growth direction is indicated by an arrow in all figures. Microanalysis was also carried out on a plane parallel to the growth direction. Microanalysis was carried out using an accelerating voltage of 10 keV. This results in a small interaction volume and a lateral spatial resolution of 1 μm can be achieved.

3 Results

3.1 Growth kinetics

Continuous directed oxidation was observed in the temperature interval of 1100°C–1400°C. Three example weight gain plots are shown in Fig. 1. For all three temperatures there was a characteristic incubation period of no growth (or possibly a very low level of oxide growth). This was followed by a period of rapid oxide growth during which the characteristic interconnected microstructure formed. If the oxidation took place at 1100°C–1300°C, this rapid oxidation continued until all the parent alloy was exhausted. However, when directed oxidation occurred at 1400°C, rapid growth would occur for only a comparatively short period before arrest leaving a substantial fraction of the Al alloy beneath a thick oxide crust.

The incubation period varied considerably from experiment to experiment (Fig. 1) but a general trend could be seen with shorter and more consistent incubation periods occurring at higher growth temperatures. The incubation period was also seen to be affected by other experimental variables such as the surface roughness of the alloy ingot before oxidation and any preheating to temperatures below 1100°C prior to directed oxidation. Incubation periods before the onset of directed oxidation have been reported by Sindel *et al.*,[4] Nagelberg[9,10,12] and Salas *et al.*,[8] all working on the Al–Mg–Si alloy system. Salas,[8] in a detailed TGA study, found a period of rapid but short duration oxide growth during the incubation period. Salas *et al.*[8] carried out a microstructural study of the oxidising surface during the incubation period and demonstrated that it was associated with the development of Al metal intrusions in a spinel ($MgAl_2O_4$) surface oxide layer. These intrusions are believed to evolve into the Al channels found in the directed oxidation product.

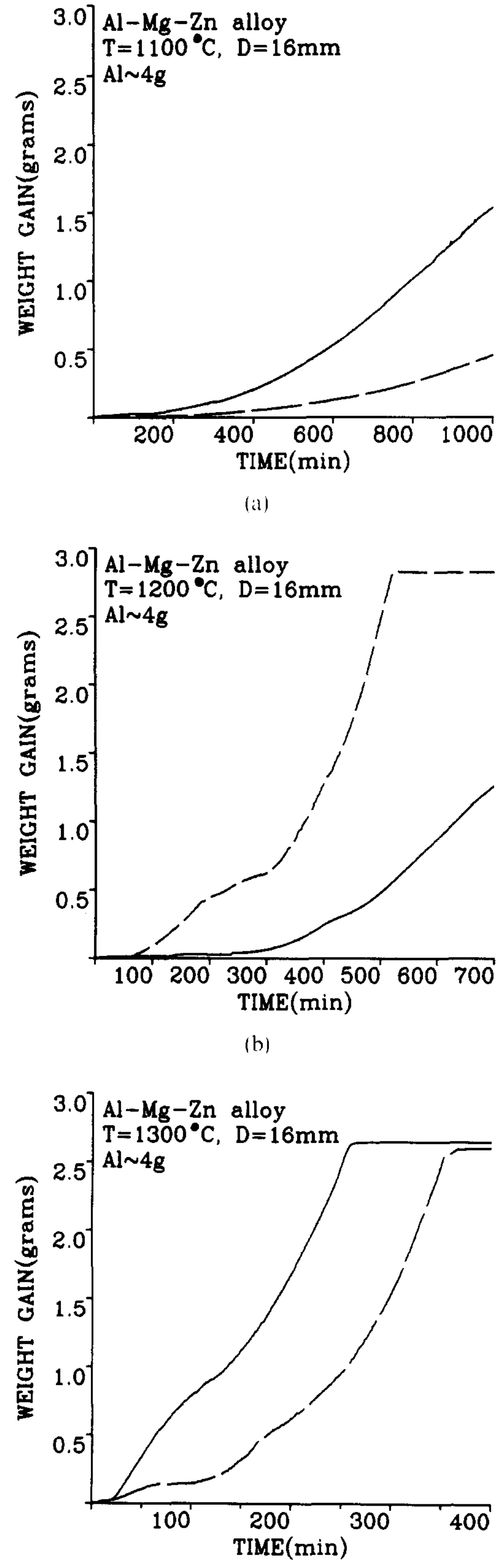

(a)

(b)

(c)

Fig. 1. Weight gain against reaction time for the oxidation of Al–Mg–Zn at: (a) 1100°C; (b) 1200°C and (c) 1300°C. Two representative experiments are shown at each temperature.

After the incubation period directed oxidation continued until the Al alloy was exhausted at temperatures from 1100°C to 1300°C. The oxide growth rate in this period increases with increasing growth temperature (Fig. 1). At 1100°C the growth rate increases slowly with increasing time until it reaches a steady value [Fig. 2(a)]. However, the growth rate is only constant when averaged over time. There is a clear minute by minute variation in the growth rate. This changing growth rate is also seen at higher temperatures, Fig. 2(b) shows a similar behaviour at 1200°C to that shown at 1100°C but

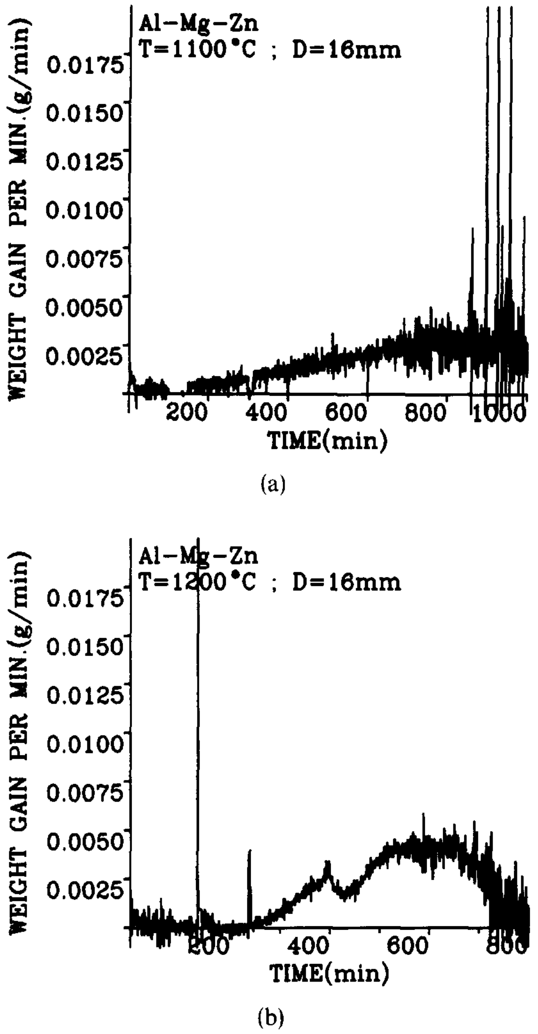

(a)

(b)

Fig. 2. Weight gain rate against reaction time for the oxidation of Al–Mg–Zn at: (a) 1100°C; (b) 1200°C.

now the mean growth rate itself varies significantly with increasing time. This variation in growth rate over a short time period is also evident in some of Nagelberg's published results.[9,10]

3.2 Product microstructures

Directed oxidation was carried out to form Al_2O_3/Al composites several millimetres thick. Oxidation did not nucleate and grow as a planar front. Instead a distinct nodular growth structure was observed with oxidation nucleating at several points on the liquid alloy surface. These nuclei impinged to form a continuous layer which was approximately planar. All the microstructures observed had many similar characteristics with two interconnected, interpenetrating networks of an Al alloy and the Al_2O_3 oxide product. It is important to realise that the oxide product grows up, or away from the initial alloy/air interface, into the oxidant (in this case air). Thus microstructures from different positions within the oxide reflect conditions at different periods of growth. For future discussion we define the 'top' of the product as material from close to the product/air interface which represents the final stages of oxidation of the sample. The 'bottom' of the sample indicates material taken from close to the alloy/product interface which represents oxidation products formed during incubation or during the very first stages of growth after incubation. The 'middle' of the sample represents material grown during the directed oxidation process in general.

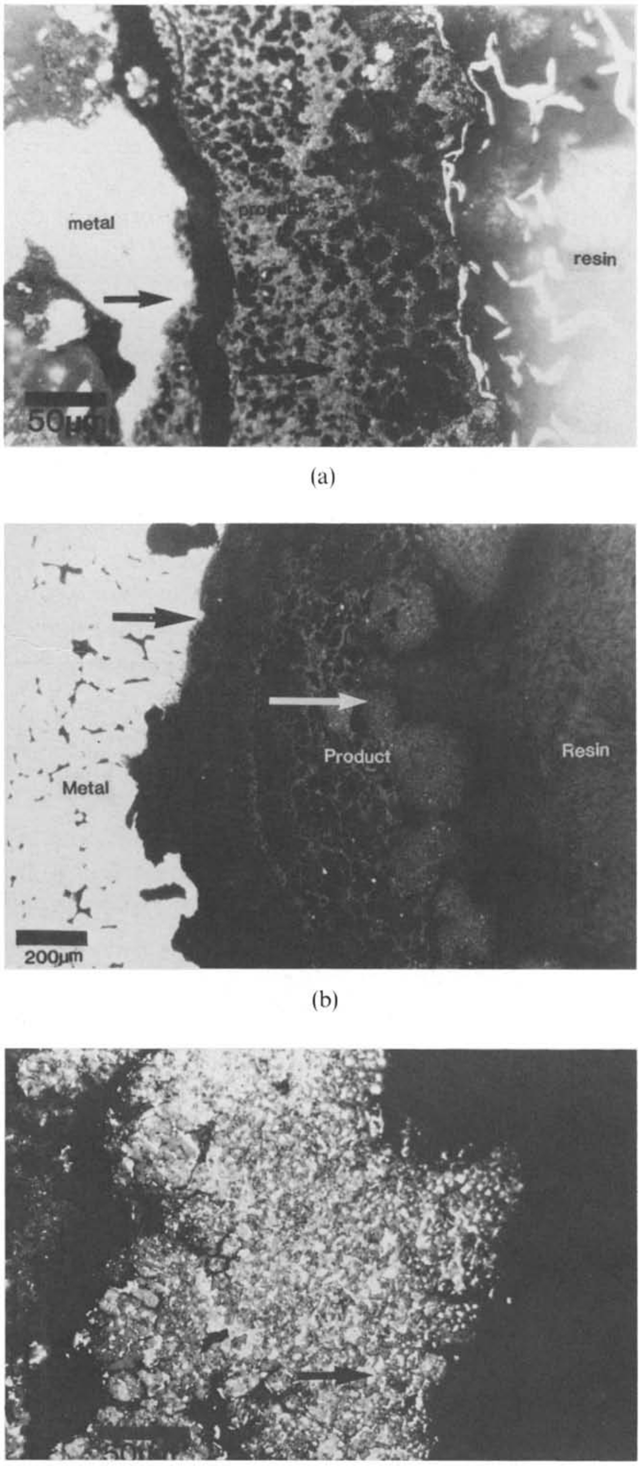

(a)

(b)

(c)

Fig. 3. Microstructure of the directed oxidation product from Al–Mg–Zn grown at 1200°C. (a) Top surface after 2 h growth (during the incubation); (b) top surface after 4 h growth (after the incubation); (c) higher magnification image of the top surface after 4 h showing composite microstructure. Arrows indicate growth direction.

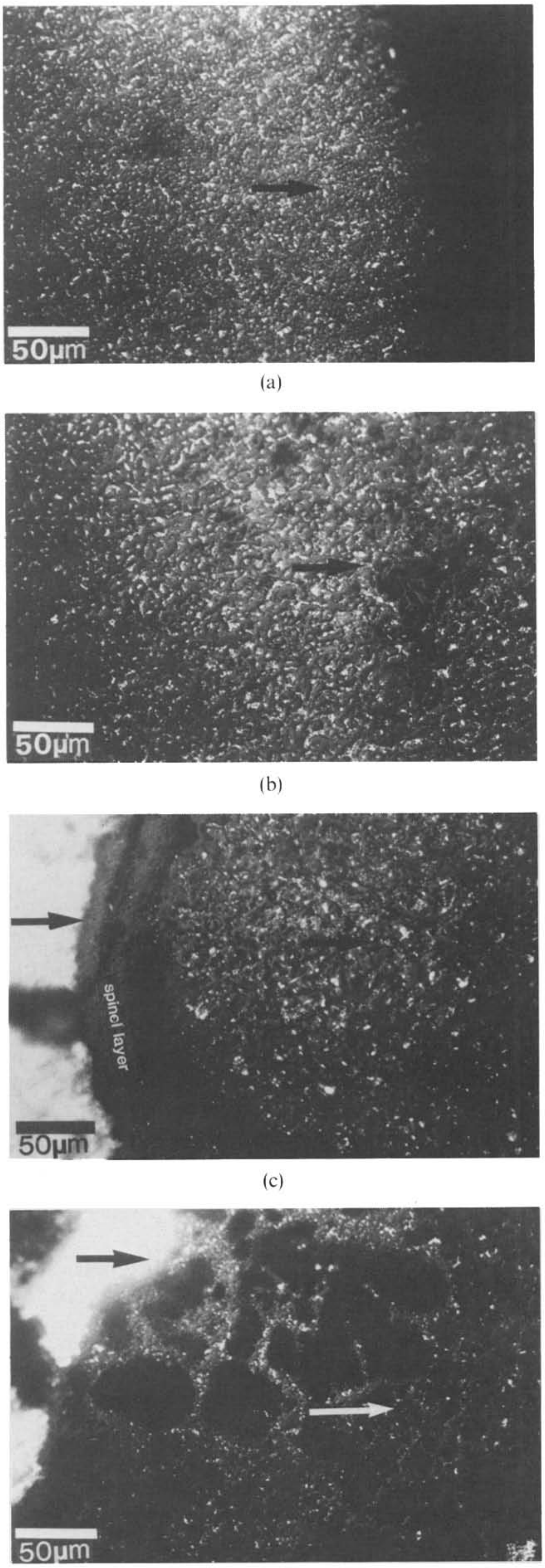

Fig. 4. Microstructure from an Al–Mg–Zn alloy oxidised at 1200°C, from: (a) top; (b) middle; (c) bottom of the specimen; (d) similar area to (c), but now extensive porosity is seen. Arrows indicate growth direction.

Figure 3 shows microstructures from the Al–Mg–Zn alloy during and just after incubation at 1200°C. Figure 3(a) shows a cross-section of the top surface after 2 h incubation. A porous oxide structure is seen which has a thickness varying from about 10 μm to a few hundred μm at different positions along the surface of the alloy. WDS microanalysis identified this as a duplex oxide layer consisting of MgO at the top surface in contact with air and $MgAl_2O_4$ just below it in contact with the alloy. Figure 3(b) shows a similar area of the sample after 4 h at 1200°C. There are now two layers of different contrast, one touching the alloy and the other near the top surface. Higher magnification images show a characteristic duplex interconnected microstructure identified as Al and Al_2O_3 by microanalysis.

In order to compare specimens grown under different experimental conditions at an equivalent stage of the process, oxidation was stopped after 1 g of weight gain for a number of specimens. Figure 4 shows one such specimen oxidised at 1200°C. The mean Al channel size is slightly smaller at the top of the specimen than at the bottom. There is a continuous layer of a phase identified as $MgAl_2O_4$ by EDS microanalysis [Fig. 4(c)] at the product alloy interface. This layer is not continuous across the entire interface and areas of high porosity [Fig. 4(d)] were often found when the spinel layer was absent.

Figure 5 shows the microstructures of a specimen produced at 1300°C. Now there is an even greater difference between Al channel size at the top and bottom of the product. The channels near the top surface are also much smaller than those found in the same position in the 1200°C product [Fig. 5(a)]. There is considerably more porosity at 1300°C which is, as with the 1200°C product, mostly found towards the bottom of the specimen, near the original alloy/air interface.

Oxidation at 1400°C only results in a comparatively thin layer of the reaction product on the top surface (Fig. 6). This contains no Al channels and shows no porosity.

3.3 Elemental distribution

During the incubation period a film forms along the metal surface prior to the onset of directed oxidation. Figure 7(a) shows WDS microanalysis traces from a cross-section of a specimen held for 2 h at 1200°C. A duplex oxide film is seen, with MgO exposed to the atmosphere and a $MgAl_2O_4$ (spinel) layer between it and the liquid metal. A significant segregation of Mg seems to occur within the liquid metal. Figure 7(b) is a microanalysis scan of the unreacted Al alloy beneath the surface oxide film. In the region just below the oxide film there is a significant increase in Mg content up to about 2·9%

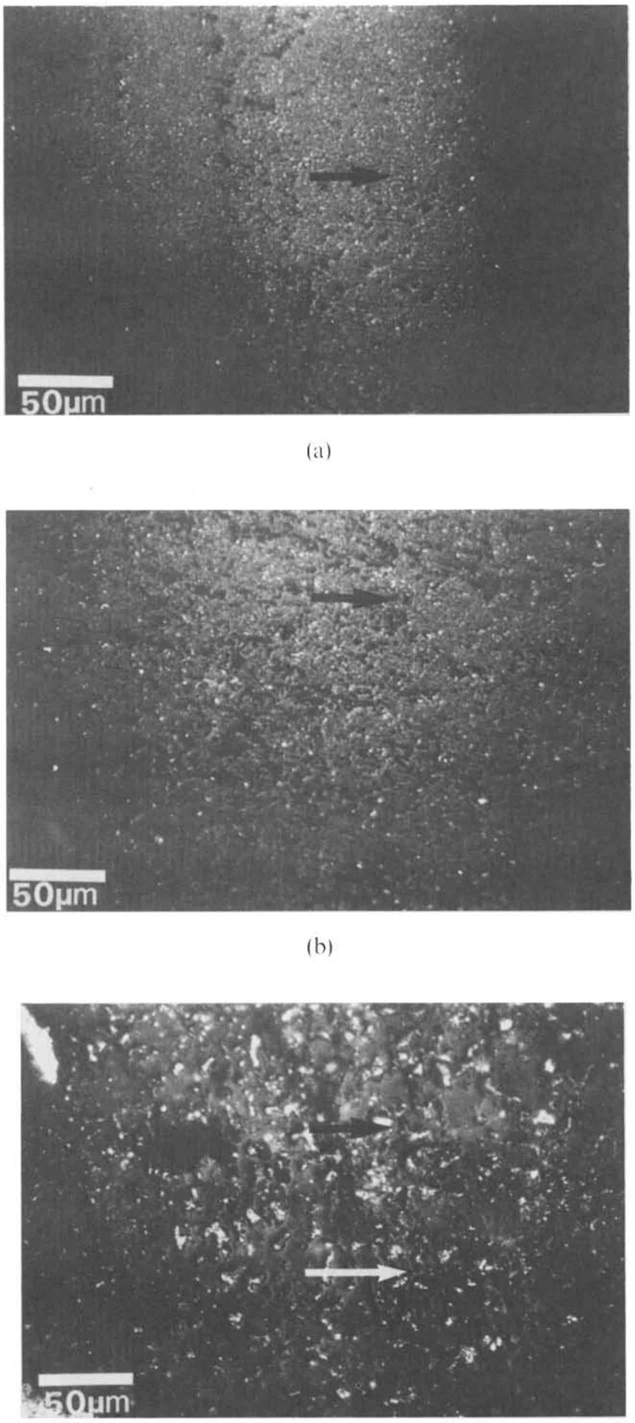

(a)

(b)

(c)

Fig. 5. Microstructure from an Al–Mg–Zn alloy oxidised at 1300°C, from: (a) top; (b) middle; (c) bottom of the specimen. Arrows indicate growth direction.

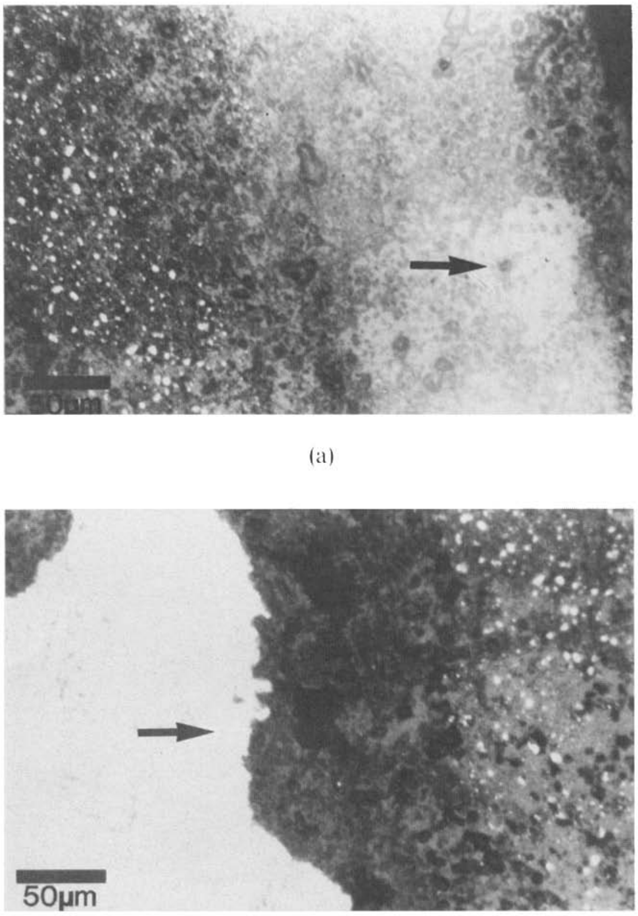

(a)

(b)

Fig. 6. Microstructure from an Al–Mg–Zn alloy oxidised at 1400°C, from: (a) top; (b) bottom of the specimen. Arrows indicate growth direction.

from the original 2·2%. However, from about 20 µm into the alloy the Mg content of the rest of the Al alloy falls to below that of the original level.

After the incubation period directed oxidation begins. Figure 8(a) shows a WDS line-scan across the metal/reaction product interface after oxidation to 1 g weight gain in air at 1200°C. The MgO and $MgAl_2O_4$ layers formed during incubation are still present with the Al_2O_3/Al composite growing on top. Figure 8(b) shows a SEM image of the top surface of the sample in cross-section with a Mg line trace superimposed. It was not possible to get quantitative composition data so close to the surface, but a clear increase in Mg content could be observed. Figure 8(c) shows the Mg content of the residue of the parent alloy after 1 g had been oxidised. As in Fig. 8(c) there has been a significant decrease in the Mg level of the alloy at distances greater than about 40 µm from the first oxidation product.

By using very low accelerating voltages in a dedicated microprobe and applying ZAF correction routines we are able to produce high resolution X-ray microanalyses with a spatial resolution of about 1 µm. Hence a number of spot analyses were carried out to investigate the composition of the metal in the Al_2O_3/Al product microstructure (Table 1). Note that the Mg content of the metal channels is very low indeed with a slightly higher concentration near the ceramic/air interface. The Zn content is slightly higher than in the parent alloy which may be caused by some form of solute rejection. If the reaction was allowed to run until all the metal was exhausted, a fine powdery deposit was found on the top surface of the product after removal from the furnace. This was

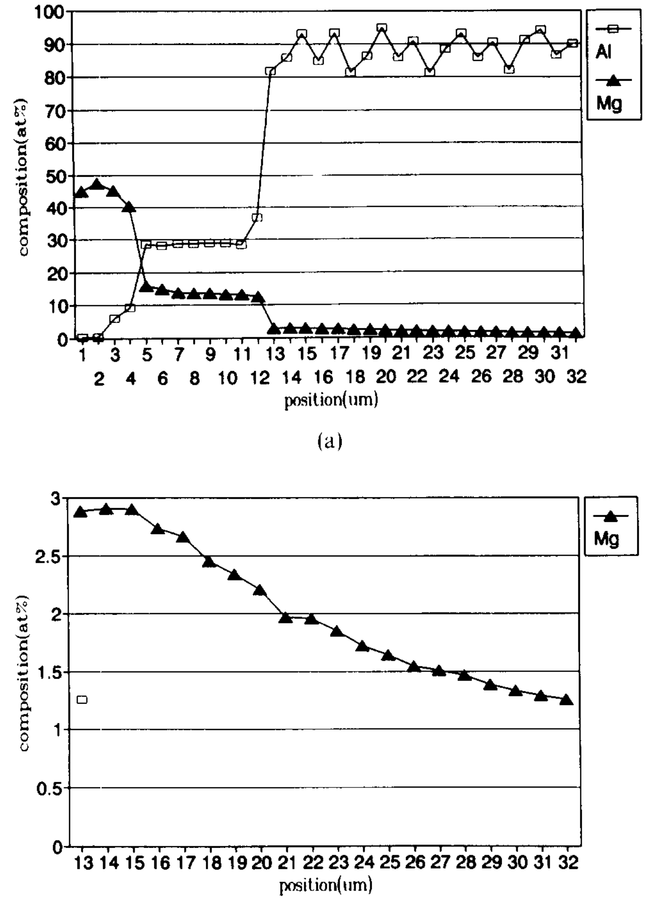

(a)

(b)

Fig. 7. Microanalysis line scans from an Al–Mg–Zn specimen oxidised for 2 h at 1200°C (during the incubation). (a) Top surface showing MgO and $MgAl_2O_4$ layers; (b) Mg concentration in the metal below the oxide film. The position indicates distance from the original metal/air interface.

identified as ZnO by X-ray diffraction. ZnO was never found other than after the complete oxidation of the Al.

At 1400°C and 1500°C no directed oxidation occurred even after 24 h exposure to temperature. In these materials the parent alloys were examined using the electron microprobe and both their Mg and Zn alloy contents had fallen to below 0·1 at%.

Table 1. Microprobe results from locations in an Al/Al_2O_3 composite produced by the directed oxidation of Al–Mg–Zn alloy at 1200°C for 7 h

Position	*Mg at %*	*Zn at %*	*Si at %*
Parent alloy	2·16	2·2	<0·3
Channel near ceramic/ air interface	0·5	2·7	0
Channel near ceramic/ air interface	0·4	2·7	1
Channel near ceramic/ metal interface	0·2	3·9	0·2
Intermediate channel	0·3	3·3	0·4
Intermediate channel	0·2	3·5	0·3
Intermediate channel	0·2	3·6	0·3
Intermediate channel	0·2	3·5	0·3
Intermediate channel	0·3	3·3	0·3

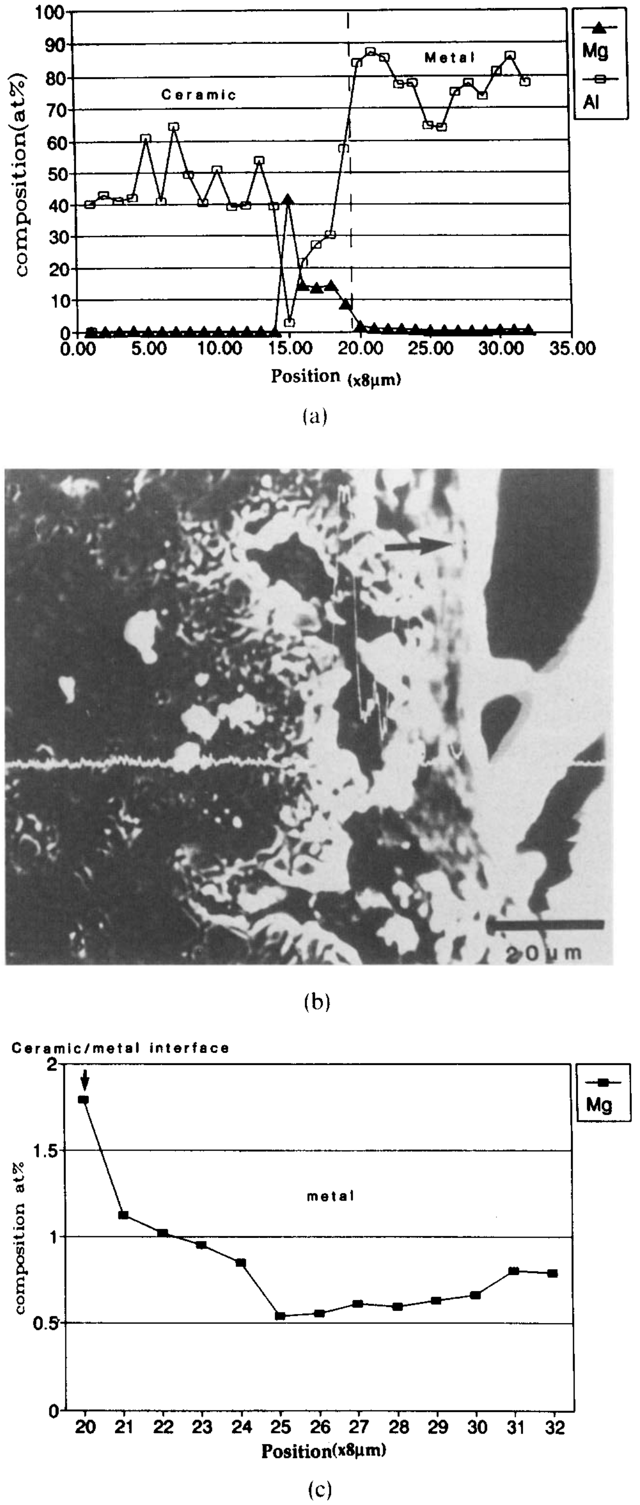

(a)

(b)

(c)

Fig. 8. (a) Microanalysis line scans across the parent metal/ceramic interface from the Al–Mg–Zn alloy reacted in air at 1200°C. Note the presence of both MgO and $MgAl_2O_4$. (b) Mg line scan superimposed on a cross-sectional SEM image of an Al_2O_3 surface grown from Al–Mg–Zn at 1200°C. Note the peak in Mg concentration near the surface. (c) Microanalysis line scan from the parent metal/ceramic interface to the middle of the parent metal, distance from the metal/ceramic interface is shown in 8 µm units.

4 Discussion

A knowledge of the various equilibria in the Al–Mg–O phase system is needed to interpret these results. The equilibria between Al–Mg alloys and the oxides Al_2O_3, $MgAl_2O_4$ and MgO were calculated

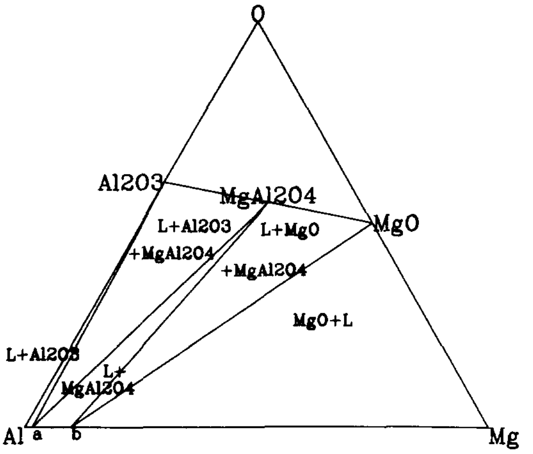

Fig. 9. Isothermal section of the calculated Al–Mg–O phase diagram at 1200°C. (a) = 0·18 at%. (b) = 9·98 at%.

in an earlier report.[13] This is used in Appendix 1 to determine isothermal sections of the Al–Mg–O equilibrium diagram. The section at 1200°C is given in Fig. 9. From Fig. 9 and Table 2, the concentration of Mg present in the Al channels (0·2 at%) is close to the predicted equilibrium level of an Al–Mg alloy in contact with Al_2O_3. This is in keeping with other reports[14,15] which show that $MgAl_2O_4$ forms if higher Mg content alloys are brought into contact with Al_2O_3 when liquid. Thus, whatever the detailed function of Mg in promoting directed oxidation, only very low levels are transported to the oxidising surface via the liquid metal channels.

A number of directed oxidation experiments were interrupted and the Al_2O_3/Al product cap removed. All the remnant Al metal was leached out using a concentrated NaOH solution to produce a porous Al_2O_3 body which had a thin duplex $MgO/MgAl_2O_4$ layer along its bottom surface. These porous Al_2O_3 samples were repeatedly washed in water and ultrasonically cleaned to remove the NaOH. Subsequently the caps were placed on top of 99·9% pure Al specimens and returned to the furnace at 1200°C. These caps were able to induce directed oxidation in these pure Al specimens without a nucleation period and produced composite microstructures broadly similar to those produced by the alloy (compare Figs 3 and 10). Thus

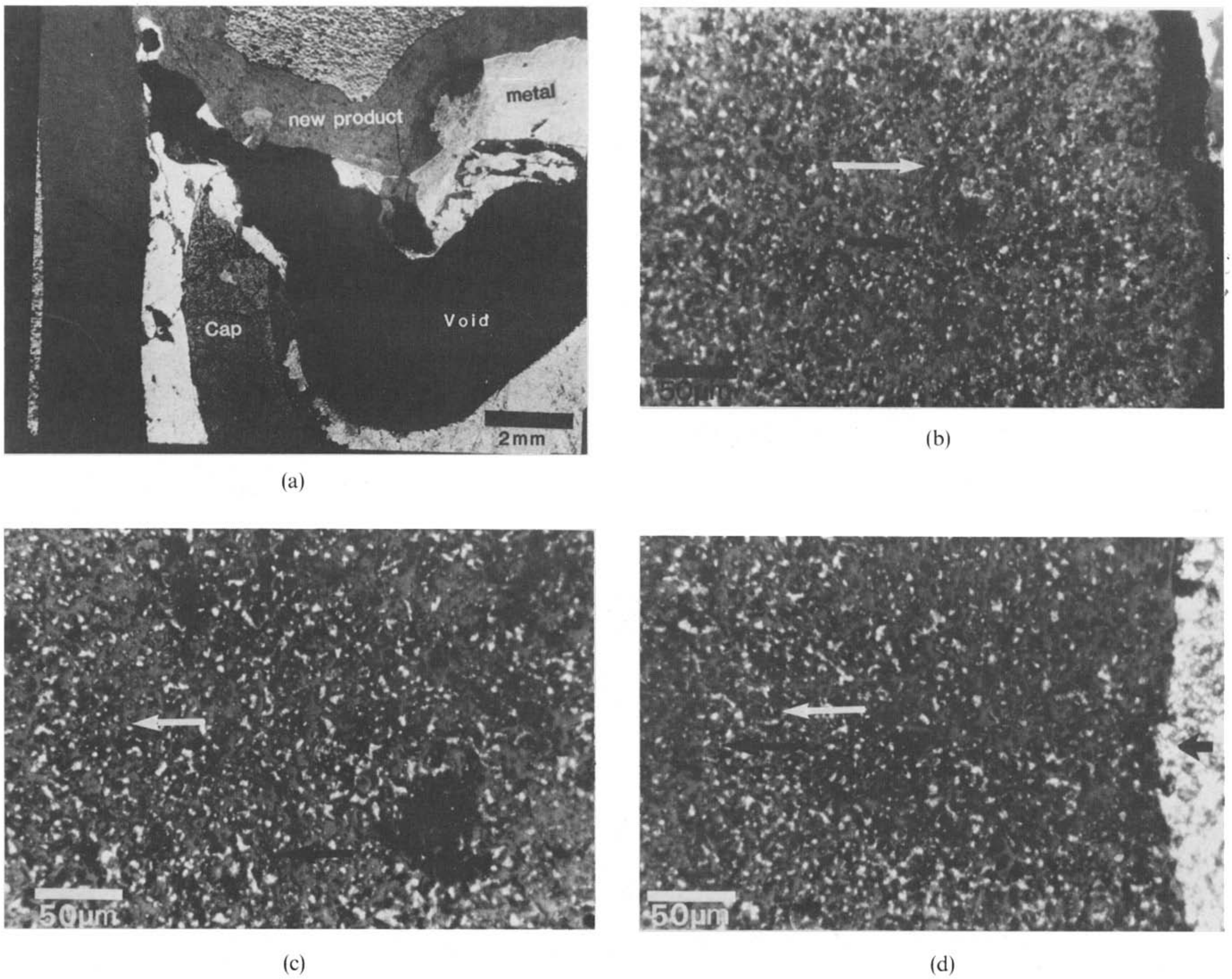

(a)

(b)

(c)

(d)

Fig. 10. Microstructure of the specimen from oxidation of pure Al capped with the product of the Al–Mg–Zn alloy. (a) Overall section, a large void has appeared in the middle of this specimen; (b) near the top surface; (c) from the middle of the product; (d) near the bottom surface. Arrows indicate growth direction.

it would appear that either the Mg concentration at the top of the specimen [Fig. 8(b)] or the $MgO/MgAl_2O_4$ layer at the parent metal/product interface [Fig. 8(a)] is all that is necessary to control the reaction. Hence a further series of experiments were carried out with the leached Al_2O_3 caps.[13] Now either the top surface of the cap (Mg rich) or the bottom surface (with the $MgO/MgAl_2O_4$ layer) was machined off before its use as a starter for the directed oxidation of pure Al. The results were inconclusive. If the Mg rich top surface was removed and the spinel containing surface placed in contact with the Al, directed oxidation always occurred. If the spinel containing surface was removed and the porous Al_2O_3 placed in contact with the alloy but with the Mg rich surface exposed to air, oxidation occurred in most but not all cases. However, if both sources of Mg were removed by machining away the top and bottom surfaces the remaining porous Al_2O_3 never induced directed oxidation of pure Al.

Further evidence for the role of Mg in promoting directed oxidation can be inferred from the parallel change in microstructure of the oxide product and Mg content of the parent alloy. In all cases there is a change in metal channel size with time at reaction temperature. This change is accompanied by a decrease in the parent alloy Mg content. When a leached Al_2O_3 cap is used to induce directed oxidation the resulting microstructure (Fig. 10) is similar to that found in the later stages of alloy oxidation (Fig. 4). Mg loss by evaporation will occur more rapidly at 1300 C which explains the greater change in channel size seen in Fig. 5. The reduction in Mg content by evaporation above 1400°C has become so rapid that no directed oxidation can occur before the Mg content falls below some critical level.

The incubation period appears to be controlled by the growth and penetration of a $MgO/MgAl_2O_4$ oxide film as proposed by Salas *et al.*[8] However, no period of early rapid oxide growth was detected, unlike the results of Vlach *et al.*[11] The variable length of incubation period and the nodular early growth morphology implies that the nucleation of the process is relatively difficult but as the variation and duration of this incubation is decreased at higher temperatures it is probably temperature activated. The nodular growth will also explain variations in reaction rate as measured by weight gain because weight gain will be proportional to the area exposed to oxidant and hence sensitive to changes in area during nodule growth and coalescence. It has been found that directed oxidation can occur with no incubation period if a starter Al_2O_3 cap is used. This is also true if, instead of a Mg-containing Al alloy, MgO is applied to the surface of a pure Al melt[19] or if NaOH is used in a similar way.[20] Thus both MgO and NaOH were used as surface dopants on the Al–Mg–Zn alloy to suppress incubation in this study. The addition of NaOH reduced incubation time at 1200°C to zero, however, the addition of MgO had no apparent effect (Fig. 11). The mechanisms which generate this incubation behaviour still need further study.

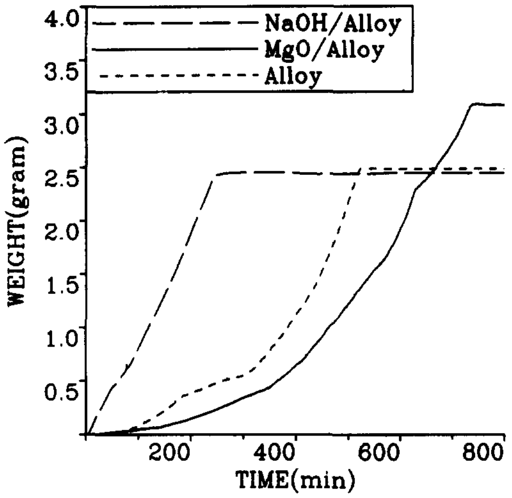

Fig. 11. Weight gain against reaction time in the oxidation of an Al–Mg–Zn alloy at 1200 C doped with MgO powder and NaOH.

The mechanism which leads to this directed oxidation behaviour is far from clear. Both Baum *et al.*[21] and Nagelberg[9] propose a mechanism which requires the presence of a MgO film above a very thin layer of liquid Al, which in turn covers the growing Al_2O_3 surface. The mechanisms require complex diffusional transport processes in the MgO film to explain the experimental observations. However, phase diagram and equilibrium data shown in Fig. 9[14,15] indicate that it would be impossible to have a Mg-containing Al melt simultaneously in equilibrium with MgO and Al_2O_3. This is also unlikely as our measurements of the alloy composition close to the surface of $<0{\cdot}5$ at% Mg could not be in equilibrium with MgO. Thus if a solid surface oxide film exists it is more likely to be of composition $MgAl_2O_4$ or else of duplex $MgO/MgAl_2O_4$ composition as proposed by Salas.[8] The transport of Mg to the top surface occurs via the low Mg content ($<0{\cdot}2$ at% Mg) of the Al metal channels. The very small buildup of Mg just below the composite air interface indicates a loss of Mg because no Mg-containing phases are found in the ceramic. The spinel layer between the unreacted alloy and the composite will be stable at alloy compositions $0{\cdot}2\,at\% < Mg < 10\,at\%$. This layer acts as a buffer ensuring the constant supply of Mg to the reacting surface.

Two final phenomena remain unexplained. First the short-term variation in oxidation rate seen in Fig. 2 and second the porosity which occurs with increasing reaction temperature. The first phenomenon may be caused by a continually varying reaction surface area or by the mechanism not reflecting a true steady state surface condition. The second phenomenon of voids in the composite microstructure could occur if the liquid transport to the growth front is controlled independently from the reaction rate. Thus an imbalance in liquid metal supply could lead to the void formation.

5 Conclusion

Directed oxidation occurs in an Al-2·2 at% Mg-2·2 at% Zn alloy showing many similarities to the behaviour of Al–Mg–Si alloys. Oxide growth occurs in the temperature interval $1100°C < T < 1400°C$ with the upper temperature controlled by the rate of Mg loss from the system. The reaction is controlled by the presence of a Mg concentration at the composite/air interface. Mg content in a network of molten Al feeder channels is maintained at 0·2 at% Mg with a thick spinel layer at the alloy/Al_2O_3 interface acting as a controlling buffer. Considering the equilibria possible at 1200°C it is likely that any Mg containing surface oxide film is of composition $MgAl_2O_4$.

References

1. Newkirk, M. S., Urquhart, A. W., Zwicker, H. R. & Breval, E., Formation of lanxide ceramic composite materials. *J. Mater. Res.*, **1** (1986) 81.
2. Aghajanian, M. K., MacMillan, N. H., Kennedy, C. R. & Luszcz, J., Properties and microstructures of lanxide Al_2O_3-Al ceramic composite materials. *J. Mater. Sci.*, **24** (1989) 658.
3. Nagelberg, A. S., Observation on the role of Mg and Si in the directed oxidation of Al–Mg–Si alloys. *J. Mater. Res.*, **7** (1992) 265.
4. Sindel, M., Travitzky, N. A. & Claussen, N., Influence of Mg–Mg spinel on the directed oxidation of molten Al alloys. *J. Am. Ceram. Soc.*, **73** (1990) 2615–18.
5. Antolin, S. & Nagelberg, A. S., Formation of Al_2O_3/metal composites by the directed oxidation of molten Al–Mg–Si alloys. *J. Am. Ceram. Soc.*, **75** (1992) 447–54.
6. Breval, E., Aghajanian, M. K. & Luszcz, S. J., Microstructure and composition of alumina/aluminium composites made by directed oxidation of aluminium. *J. Am. Ceram. Soc.*, **73** (1990) 2610–14.
7. Newkirk, M. S., Lesher, H. D., White, D. R., Kennedy, C. R., Urquhart, A. W. & Claar, T. D., Preparation of lanxide ceramic matrix composites: matrix formation by the directed oxidation of molten metals. *Ceramic Engineering and Science Proceedings*, **8** (1987) 879.
8. Salas, O., Ni, H., Jayaram, V., Vlach, K. C., Levi, C. G. & Mehrabian, R., Nucleation and growth of Al_2O_3/metal composites by oxidation of aluminum alloys. *J. Mater. Res.*, **6** (1991) 1964.
9. Nagelberg, A. S., Growth kinetics of Al_2O_3/metal composites from a complex aluminium alloy. *Solid State Ionics*, **32/33** (1989) 783–8.
10. Nagelberg, A. S., The effect of processing parameters on the growth rate and microstructure of Al_2O_3/metal matrix composites. *Proc. MRS Symp.*, **155** (1989) 275.
11. Vlach, K. C., Salas, O., Ni, H., Jayaram, V., Levi, C. G. & Mehrabian, R., A thermogravimetric study of the oxide growth of Al_2O_3/Al alloy composites. *J. Mater. Res.*, **6** (1991) 1964.
12. Nagelberg, A. S., Antonlin, S. & Urquhart, A. W., Growth kinetics for the formation of Al_2O_3/metal composites by the directed oxidation of molten aluminum alloys. *J. Am. Ceram. Soc.*, **75** (1992) 455–62.
13. Xiao, P. & Derby, B., The formation of Al_2O_3/Al composites by controlled oxidation of Al. In *Surfaces and Interfaces*, ed. R. Morrell & G. Partridge. *Proc. Brit. Ceram. Soc.*, **48** (1991) 153–60.
14. Weierauch, D. A. Jr, Interfacial phenomena involving liquid metals and solid oxides in the Mg–Al–O system. *J. Mater. Res.*, **3** (1988) 729–39.
15. Hallstedt, B., Liu, Z. K. & Agren, J., Fibre-matrix interactions during fabrication of Al_2O_3–Mg metal matrix composites. *Mater. Sci. Eng.*, **A129** (1990) 135–45.
16. *Smithells Metal Reference Handbook* (6th edn). Butterworth, Oxford, 1983.
17. Tiwari, B. L., Thermodynamic properties of liquid Al–Mg alloys measured by the emf method. *Metall. Trans.*, **18A** (1987) 1645.
18. Ludecke, D. & Hack, K., A thermodynamic evaluation of the Al–Mg system. *Z. Metallkde*, **77** (1986) H3.
19. Xiao, P. & Derby, B., Alumina/aluminium composites formed by the directed oxidation of aluminium using magnesia surface dopants. *J. Amer. Ceram. Soc.* (submitted).
20. Xiao, P. & Derby, B., Alumina/aluminium composites formed by the directed oxidation of aluminium using a sodium hydroxide surface dopant. *J. Amer. Ceram.* (submitted).
21. Baum, L., Shafry, N. & Brandon, D. G., The growth mechanism for Al_2O_3 prepared by controlled melt oxidation. Presented at CIMTEC June 24–30, 1990, Montecatini, Terme, Italy.

Appendix: Equilibria in the Al–Mg–O System

There are three possible oxide phases of the Al–Mg–O system in equilibrium with melts: alumina (Al_2O_3), magnesia (MgO), and spinel ($MgAl_2O_4$). The standard free energies and the enthalpies of formation are respectively given in Table A1.[16]

$\Delta G°f298K$ and $\Delta H°f298K$ are the standard free energy and enthalpy change of formation of the oxide per mole of oxygen at 298K(To) and are abbreviated as $\Delta G(To)$ and $\Delta H(To)$. The standard free energies of formation of oxides at different temperatures $\Delta G°fa(T)$ can be calculated from $\Delta G(To)$ by the Gibbs-Helmholtz equation.

For the formation of the oxides from liquid Al–Mg alloys, the Gibbs free energies of formation $\Delta Gfa(T)$ are given as:

$$\Delta Gfa(T) = \Delta G°fa(T) + RT \ln X_{Al} X_{Mg} + \Delta G^E \tag{A1}$$

$$a = \tfrac{1}{3}Al_2O_3,\ MgO \text{ or } \tfrac{1}{4}MgAl_2O_4$$

Table A1. The standard free energies and the enthalpies of formation of the oxides present in the Al–Mg–O system

	$\frac{1}{3}Al_2O_3$	MgO	$\frac{1}{4}MgAl_2O_4$
$-\Delta G°f$ (298 K) kJ mol^{-1}	382·3	571·1	547·9
$-\Delta H°f$ (298 K) kJ mol^{-1}	559·4	601·6	578·8

Table A2. Thermodynamic data for use in eqn (A2)

v	A	B
0	−10 243·4	4·944 6
1	7 328·6	−9·014 6
2	2 412·2	−0·025 1

The thermodynamic properties of liquid Al–Mg alloys have been determined by emf methods.[17] Experimental thermodynamic information has been used in deriving a thermodynamically consistent analytical description. Excess Gibbs energy of mixing ΔG^{E} in the liquid Al–Mg solution is represented by a Redlich-Kister polynomial (in J mol^{-1}).[18]

$$\Delta G^{\mathrm{E}} = XiXj(Xi - Xj)^{v} Lij(v)(T)\,\mathrm{J\,mol^{-1}} \qquad \text{(A2)}$$

with

$$Lij = A + BT \quad (i = \mathrm{Al},\ j = \mathrm{Mg})$$

where Xi and Xj are the molar fractions and A and B are given in Table A2.

The relative stabilities of oxides can be obtained from the standard free energies of formation and the excess Gibbs energy at different compositions of Al–Mg alloys by eqn (A1). The predicted isothermal section of the Al–Mg–O ternary system phase diagram at 1200°C is shown in Fig. 9. It can be clearly seen that Al_2O_3 is only stable in contact with alloys of very low Mg content and that in general spinel is the most stable oxide phase for melts of Mg contents 0·18 at% < Mg < 9·98 at% at 1200°C.